DOI: 10.1002/chem.200501081

Control of Metal-Ion Composition in the Synthesis of Ternary II-II′-VI Nanoparticles by Using a Mixed-Metal Cluster Precursor Approach

Marty W. DeGroot,[a] Harald Rösner,[b] and John F. Corrigan*[a]

Abstract: The ternary molecular nanoclusters $[Zn_xCd_{10-x}Se_4(SePh)_{12}(PnPr_3)_4]$ ($x=1.8$, **1a**; $x=2.6$, **1b**) were employed as single-source precursors for the synthesis of high-quality hexagonal $Zn_xCd_{1-x}Se$ nanocrystals. The tellurium clusters $[Zn_xCd_{10-x}Te_4(TePh)_{12}(PnPr_3)_4]$ ($x=1.8$, **2a**; $x=2.6$, **2b**) are equally convenient precursors for the synthesis cubic $Zn_xCd_{1-x}E$ nanoparticles. The thermolysis of the cluster molecules in hexadecylamine provides an efficient system in which the inherent metal-ion stoichiometry of the clusters is retained in the nanocrystalline products, whilst also affording control of particle size within the 2–5 nm range. In all cases, the nanoparticles are monodisperse, and luminescence spectra exhibit emission energies close to the absorption edge. Analysis of the optical spectra and X-ray diffraction patterns of these materials indicates a metal-ion concentration gradient within the structures of the nanocrystals, with Zn^{II} ions predominantly located near the surface of the particles.

Keywords: cadmium · chalcogens · cluster compounds · nanostructures · zinc

Introduction

A landmark discovery in the synthesis of II-VI nanoparticles was the establishment of the trioctylphosphine/trioctylphosphine oxide (TOP/TOPO) method by Bawendi et al., affording synthetic access to high-quality, monodisperse nanoparticles in gram-scale quantities.[1] Nucleation and growth of nanoparticles in these systems are prompted by the rapid injection of metal and chalcogen precursors into a hot (~150–350 °C), coordinating solvent. The concept of pyrolytic degradation of organometallic precursors that forms the basis of the TOP/TOPO method has been complemented by numerous studies involving the use of single-source precursors in the synthesis of semiconductor nanoparticles.[2–4] This approach involves the pyrolysis of complexes with a preformed metal–nonmetal bond, tendering the potential advantages of low-temperature synthetic routes, the avoidance of toxic and volatile precursors, and low incorporation of impurities.[5,6] An expansion of this precursor approach involves the use of cluster complexes as single-source precursors to nanoparticle formation.[7,8]

Recently, Strouse and co-workers fashioned a convenient synthetic route for the synthesis of II-VI nanoparticles by combining the concept of cluster precursors with the tunability of lyothermal degradation techniques, such as the TOP/TOPO method.[9] The clusters, $[M_{10}Se_4(SPh)_{16}]^{4-}$ (M = Zn, Cd),[10] which already contain the requisite structural arrangement present in the semiconductor material, were found to be excellent candidates for nanoparticle formation. The lyothermal cluster degradation method was further extended to the synthesis of Co-doped CdSe quantum dots by using a combination of $[Cd_{10}Se_4(SPh)_{16}]^{4-}$ and $[Co_4(SPh)_{16}]^{2-}$ in hexadecylamine.[11] In a related investigation, Osterloh and Hewitt treated the tetraadamantane cadmium sulfur cluster $[Cd_{10}S_4Br_4(SR)_{12}]$ with elemental sulfur to produce crystalline wurtzite CdS with an average particle size of 5.8 nm.[12]

Among the most extensively investigated nanomaterials are those of II-VI semiconductors (M_xE_x, in which M = Zn, Cd, Hg; E = S, Se, Te), especially CdSe, for which the emission energy can be tuned across the visible spectrum.[1,13,14] Far less attention has been directed at the synthesis of ternary II-II′-VI nanoparticles. In these alloyed compounds, the

[a] M. W. DeGroot, J. F. Corrigan
Department of Chemistry
The University of Western Ontario
London, N6A 5B7 (Canada)
Fax: (+1) 519-661-3022
E-mail: corrigan@uwo.ca

[b] H. Rösner
Institut für Nanotechnologie
Forschungszentrum Karlsruhe in der Helmholtz-Gemeinschaft
Hermann-von-Helmholtz-Platz 1
76344 Eggenstein-Leopoldshafen (Germany)

Supporting information for this article is available on the WWW under http://www.chemeurj.org/ or from the author.

band gap energy can be mutually tuned by controlling both the size of the nanoparticles and the metal-ion stoichiometry (i.e. the ratio of M/M′). Indeed, recent reports on the synthesis of $Zn_xCd_{1-x}E$ and $Cd_xHg_{1-x}E$ nanoparticles demonstrate that the excitation energy of these compounds can be manipulated by changing the compositions.[15–17] Knoll and co-workers have prepared a series of highly luminescent (70–85% quantum efficiency) $Zn_xCd_{1-x}Se$ nanocrystals through the incorporation of Zn and Se into CdSe nanoparticles.[18] The emission energy of these particles can be tuned across the visible spectrum by changing the Zn/Cd ratio; the incorporation of zinc is accommodated by an increase in the size of the nanoparticle.

Recently, we reported the development of molecular precursor routes for the formation of ternary ZnCdSe and ZnCdTe nanoclusters.[19,20] These "pre-mixed" ternary cluster molecules are exceptional candidates for the synthesis of ternary nanoparticles in which the Zn/Cd ratio of the final products can be modulated by the adjustable stoichiometry of the clusters. Herein, we describe the growth of $Zn_xCd_{1-x}Se$ and $Zn_xCd_{1-x}Te$ nanoparticles from the single-source cluster precursors $[Zn_xCd_{10-x}E_4(EPh)_{12}(PnPr_3)_4]$ and $[Zn_5Cd_{11}E_{13}(EPh)_6(thf)_n(N,N'\text{-tmeda})_5]$ (E = Se, Te). This approach offers tunability both in the form of thermal control of particle size as well as in the Zn/Cd composition by variation of the metal-ion constitution of the cluster starting reagents.

Results and Discussion

Semiconductor nanocrystallites are an exciting class of materials that exist in the transition region between semiconductor solids and molecular complexes. The unique size- and surface-dependent properties of these materials have inspired a prolific development in the chemical and physical understanding of their properties.[21–27] Of particular interest from a technological standpoint are the effects of quantum confinement of the bulk exciton that result in size-tuneable optical absorption and emission properties.[28–34] As the field of "nanotechnology" has started to emerge, there has been a movement from an academic interest to one based on the implementation of these materials in electronic device applications, such as light-emitting devices,[35] photovoltaics,[36] and lasers.[37] Therefore, in addition to the control of particle size and chemical composition, the focus on the development of straightforward synthetic routes to highly processable, high-purity materials with a narrow size distribution and completely derivatized surface remains at the forefront of this area of science.

Semiconductor cluster complexes can serve as molecular structural models for bulk and nanocrystalline semiconductors,[38,39] and this has established their foundation for the application of molecular clusters as single-source precursors for nanoparticle formation. In this approach, the clusters act as "seeds" for growth and, therefore, eliminate the requirement for a nucleation step that typically involves the injection of toxic precursors into hot solutions.[1,13] The ternary nanoclusters $[Zn_xCd_{10-x}E_4(EPh)_{12}(PnPr_3)_4]$ (E = Se, $x = 0.18$, **1a**; E = Se, $x = 0.26$, **1b**; E = Te, $x = 0.18$, **2a**; E = Te, $x = 0.26$, **2b**) and $[Zn_5Cd_{11}E_{13}(EPh)_6(thf)_n(N,N'\text{-tmeda})_5]$ (E = Se, $n = 2$, **3**; E = Te, $n = 1$, **4**) are thus excellent candidates for the lyothermal generation of alloyed $Zn_xCd_{1-x}E$ nanomaterials, because their synthesis is easily scalable to produce large amounts of pure cluster material in high yield.[19,20] The clusters are stable in the solid-state under inert atmosphere and can even be handled in air for short periods of time. These are important considerations for the development of a technique to produce large quantities of nanoparticles for industrial applications. In this vein, hexadecylamine (HDA) offers an affordable alternative to the more typically employed trioctylphosphine/trioctylphosphine oxide (TOP/TOPO) solvent system. The lower boiling point of the amine relative to that of TOP does not prohibit quantum-dot growth in this system, owing to the absence of the need for a high-temperature nucleation step.[9]

Growth and metal-ion composition of the ternary $Zn_xCd_{1-x}E$ nanoparticles: The addition of the ZnCdSe or ZnCdTe cluster materials to hot (120°C) HDA immediately results in the formation of yellow (Se) or deep yellow (Te) solutions. As the temperature is gradually increased, the color of the solution progressively changes from yellow to orange and red (to deep purple for $Zn_xCd_{1-x}Te$), indicating the growth of larger materials. The progress of cluster growth can easily be monitored spectroscopically by taking aliquots at various intervals and obtaining the absorption spectrum. The nanoparticles can be isolated at the desired size by cooling the reaction below the growth temperature, followed by precipitation with methanol. The isolated nanocrystalline materials are indefinitely stable under inert atmosphere; however, extended exposure to air results in a gradual deterioration of luminescence intensities. In addition, the nanoparticles can be stored in the parent hexadecylamine mixture for prolonged periods without observable effects to their spectroscopic properties.

To determine the efficiency of these cluster precursors in the synthesis of ternary nanomaterials, the relative metal-ion compositions of the ternary $Zn_xCd_{1-x}E$ nanoparticles were examined using energy-dispersive X-ray (EDX) spectroscopy. The results of these analyses indicated that the $Zn_{0.18}Cd_{0.82}$ and $Zn_{0.26}Cd_{0.74}$ stoichiometries present in clusters **1a** and **1b** remained constant throughout the lyothermal degradation process and were retained in the nanocrystalline products. For $[Zn_5Cd_{11}Se_{13}(SePh)_6(thf)_2(N,N'\text{-tmeda})_5]$ (**3**), on the other hand, EDX intensity data suggested a continual decrease in the Zn composition of the isolated nanomaterials with increasing temperature. Similar results were obtained for the tellurium materials, with preservation of the metal-ion constitution observed for the adamantoid clusters **2a** and **2b**, and partial zinc loss occurring for cluster **4**. These results suggest that structural differences play a significant role in the thermolytic pathway. Clusters **1** and **2** exhibit the characteristic[40,41] cagelike adamantane-

based architecture **I**, representative of the building blocks comprised in the extended structures of II-VI materials, while clusters **3** and **4** exhibit more condensed structures **II**.[20] Thus, for the lyothermal decomposition of clusters **1**

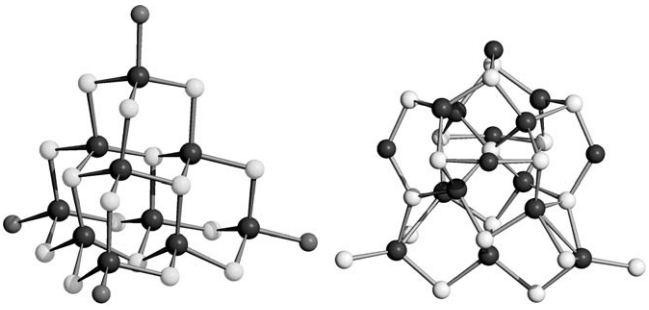

I **II**

and **2**, the composition of the resulting nanoparticles can be manipulated by controlling the metal-ion ratio of the associated cluster precursors. Our previous results have demonstrated that such stoichiometric control is easily accommodated in the synthesis of these clusters.[19] The use of clusters **3** and **4** appears to be less favorable in this regard, because the metal content of the precursors is fixed ($Zn_{0.31}Cd_{0.69}$) and the ratio of Zn/Cd changes with the thermolysis temperature.

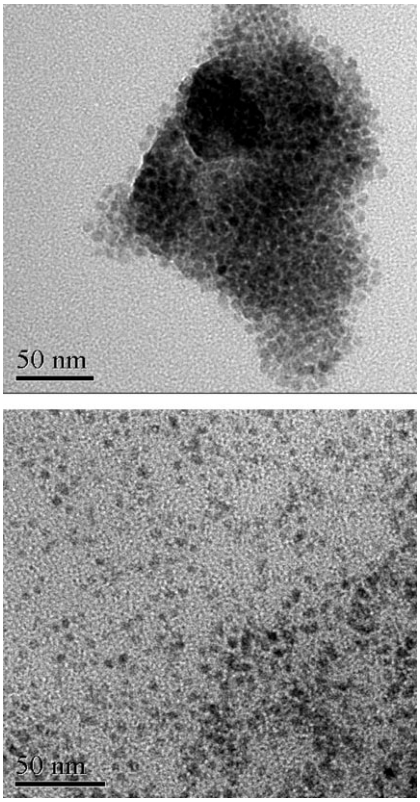

Figure 1. Bright-field TEM micrographs: Top: overview of sample **2a** heated at 240 °C in hexadecylamine. Bottom: overview of sample **2b** heated at 240 °C in hexadecylamine.

Particle-size characterization of selected ternary nanoparticles obtained from clusters **1** and **2** was carried out by using high-resolution transmission electron microscopy (TEM). The TEM micrographs verify the growth of the nanoparticles with increasing temperature, with particles attaining a maximum size of approximately 5 nm at 240 °C (Figure 1). These analyses confirmed the presence of individual nanoparticles and the highly crystalline nature of the materials, as demonstrated by the identifiable lattice fringes within the structures of the particles (Figure 2).

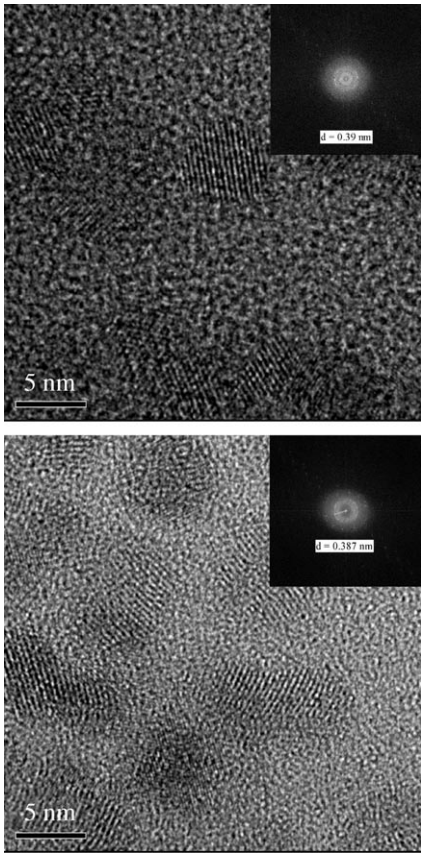

Figure 2. High-resolution TEM micrographs showing details of sample **2a** (top) and of sample **2b** (bottom) heated at 240 °C in hexadecylamine. The bar scale is 5 nm. The inserts depict the corresponding Fourier transforms; the *d*-spacing values for **2a** and **2b** calculated from the first ring of the electron diffraction pattern are 0.39 and 0.387 nm, respectively.

The evolution of particle size in the growth process of the $Zn_xCd_{1-x}Se$ and $Zn_xCd_{1-x}Te$ nanoparticles was further monitored by dynamic light-scattering analysis and by the experimentally determined (from the optical spectra, see below) band-gap energies of the semiconductor nanomaterials. These analyses revealed the following features associated with nanoparticle growth in these ternary systems. First, no substantial differences were observed between the growth of the $[Zn_xCd_{10-x}Se_4(SePh)_{12}(PnPr_3)_4]$ clusters **1a** and **1b**. Similar growth progression was also observed for the ZnCdTe clusters **2a** and **2b**. Thus, it is apparent that the small differences in the metal-ion composition of crystals of these com-

plexes have little effect on nanoparticle growth. The presence of zinc in the clusters does, however, markedly affect the growth of nanocrystalline materials at high temperature. In the synthesis of CdSe nanoparticles from the cluster $[Cd_{10}Se_4(SPh)_{16}]^{4-}$, substantial nanocluster growth is observed above 220 °C, with a two- to threefold increase (yielding 6–9 nm particles) in size observed in the 220–240 °C range.[9] For clusters **1a** and **1b** only a small increase in the growth rate is observed at this temperature, and cluster sizes reach 5 nm at 240 °C. A similar escalation of growth is observed at ~180 °C for the tellurium clusters **2a** and **2b**. The observed lower decomposition temperatures of the telluride versus selenide clusters are consistent with those of the solid-state thermolyses.[19b,20b]

Optical properties: Figure 3 shows the evolution of the absorption spectra with increasing batch temperature for the lyothermal degradation of the ZnCdSe nanoclusters **1a**,**b**.

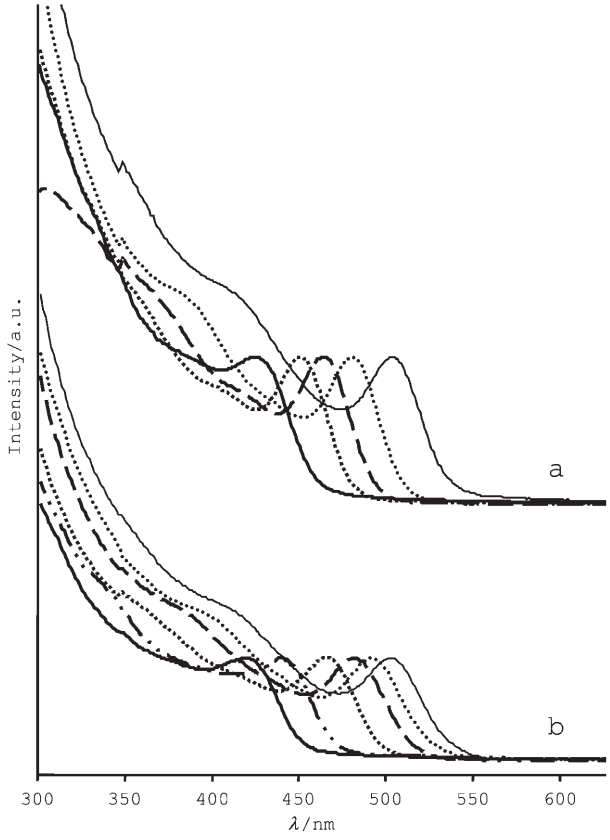

Figure 3. Normalized absorption spectra for the $Zn_xCd_{1-x}Se$ nanoparticles synthesized from clusters a) **1a** and b) **1b**. All spectra were measured at room temperature in toluene.

The absorption spectra of the nanoparticles feature well-defined absorption onsets with distinct lowest energy excitonic transitions. The sharp absorption features and the observation of higher energy second and third excitonic transitions in the absorption spectra are also indicative of a narrow size distribution.[1] Consistent with the results of related investigations,[9] this distribution could be narrowed by thermal annealing of the reaction batches at 20 °C below their growth temperature.

The effects of quantum confinement are observed as a shift of the first excitonic transition to lower energy with increasing particle size. The same effect is observed in the emission spectra (Figure 4), which have maxima at the absorption edge and line widths that are comparable to those of the absorption spectra (Figure 5). As expected these become more prominent with increasing particle size. A comparison of the optical spectra of the products obtained from clusters **1a**, **1b**, and **3** at 240 °C reveals that despite significant differences in the metal-ion content of these products, the band-gap energy of these nanoparticles is virtually identical (see Supporting Information). This feature is inconsistent with the homogeneous distribution of zinc(II) within the structure of the nanoparticles. The presence of in-

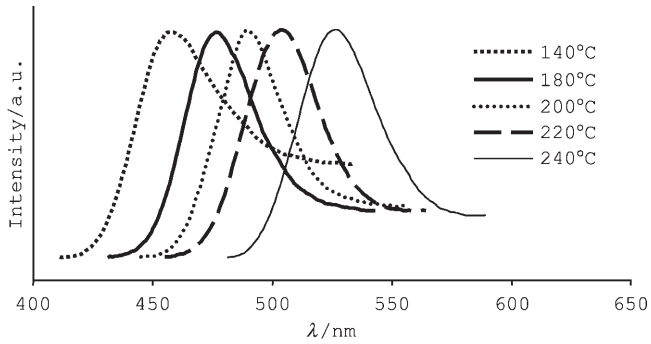

Figure 4. Normalized emission spectra for the $Zn_xCd_{1-x}Se$ nanoparticles synthesized from clusters **1b** isolated at various temperatures. The excitation wavelength for all samples was 350 nm.

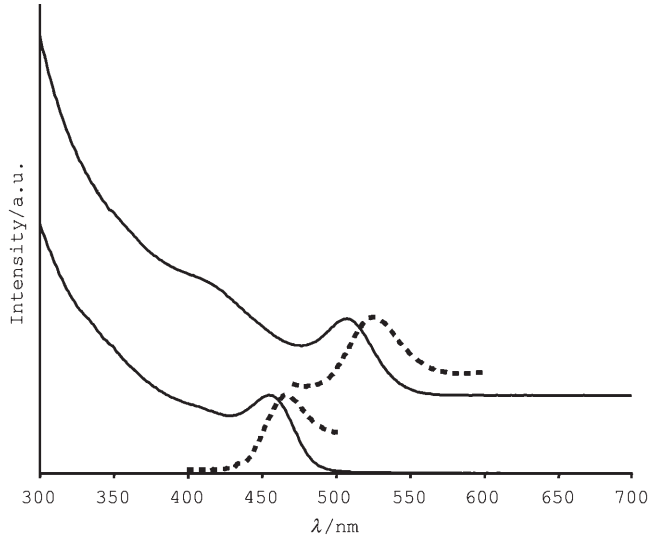

Figure 5. Comparison of the absorption (——) and photoluminescence (– – –) spectra of the ternary $Zn_xCd_{1-x}Se$ nanoparticles synthesized by means of the lyothermal decomposition of cluster **1b** isolated at 180 °C (bottom) and 240 °C (top).

dividual ZnSe and CdSe nanoparticles can be ruled out by the absorption and emission spectra, which feature optical transitions associated with a single species.

The most likely explanation is that a concentration gradient of the metal ions is present in the nanoparticles, with a majority of the zinc(II) centers residing near the quantum-dot surfaces. The relative sharpness of the absorption and emission spectra, as well as the presence of higher energy excitonic transitions is consistent with this elucidation, as mixed ternary $Zn_xCd_{1-x}Se$ nanoparticles feature broader spectra.[18] In comparison to those of the $Zn_xCd_{1-x}Se$ nanoparticles, the absorption and emission spectra of the $Zn_xCd_{1-x}Te$ derivatives are shifted to lower energy, consistent with the relative band-gap energies of the bulk semiconductors (Figure 6). Thus, the emission of these nanoparticles can be extended into the red region of the visible spectrum (Figure 7). The absorption spectra of these nanoparticles show less structure than their selenide counterparts and, in addition, the full width at half maximum height (fwhm) of the lowest energy bands of out-of-batch samples increases markedly with increasing reaction temperature, suggesting that the size distribution widens significantly as particle size increases. Again, this can be improved by thermal annealing of the batches below the growth temperature. Evaluation of the absorption and emission energies of the products from **2a**, **2b**, and **4** suggest that the Zn^{II} ion is also concentrated near the nanoparticle surfaces, similar to "type I" core/shell structures. In "type I" core/shell materials, a nanocrystalline core is covered with a shell of a wider band-gap material and these nanocrystals often exhibit increased photoluminescence efficiency and photostability relative to binary "core-only" quantum dots.[42–44] Alternatively, reverse "type II" nanoparticles, in which the narrower gap semiconductor is employed as the shell, are designed to spatially separate photogenerated charge carriers in the core and shell materials,[45] and the emission can be tuned by changing the relative thickness of the shell material.[46]

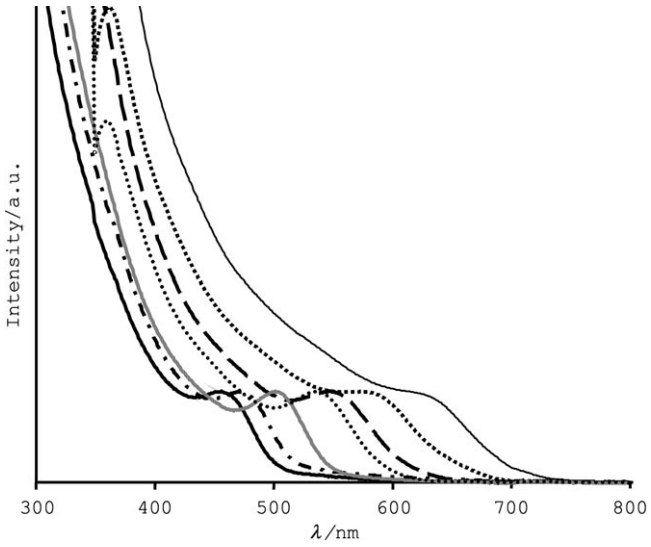

Figure 6. Normalized absorption spectra for the $Zn_xCd_{1-x}Te$ nanoparticles synthesized from clusters **2b**. All spectra were measured at room temperature in toluene.

Structural characterization: Structural analysis of the $Zn_xCd_{1-x}Se$ and $Zn_xCd_{1-x}Te$ nanoparticles was carried out by using powder X-ray diffraction (XRD; see Supporting Information). While the broadness of the XRD patterns for the selenide series prohibits unambiguous assignment of the crystal lattice type, the data are most consistent with the hexagonal (wurtzite) structure, as observed by Knoll and Han and co-workers for their TOP-capped $Zn_xCd_{1-x}Se$ nanoparticles.[18] In the $Zn_xCd_{1-x}Te$ system, XRD patterns could be indexed to the cubic (sphalerite) phase. These structural types are consistent with those observed for the solid-state thermolysis of the clusters.[19b,20b] Since the structural architectures of the cluster precursors **1a**,**b** are composed exclusively of adamantane cages that represent the fundamental unit of the cubic modification, the formation of hexagonal $Zn_xCd_{1-x}Se$ must be accompanied by a change from the adamantane to a barrelane cage structure. The evident decrease in the relative broadness of the Bragg diffraction peaks with increasing reaction temperature can be attributed to the increasing particle size.

The consistency of the peak positions in the XRD patterns of compounds with different metal composition (Figure 8) provides support that the majority of zinc ions

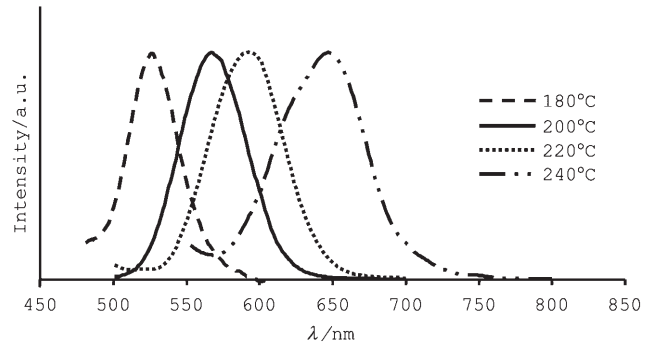

Figure 7. Normalized emission spectra for the $Zn_xCd_{1-x}Te$ nanoparticles synthesized from clusters **2b** isolated at various temperatures. The excitation wavelength for all samples was 450 nm.

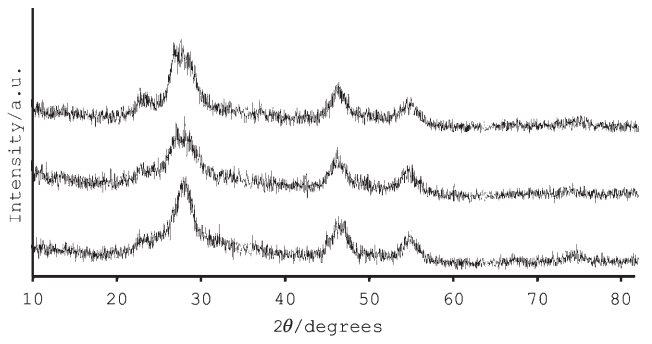

Figure 8. Powder XRD patterns for the fractions taken at 240°C for the synthesis of $Zn_xCd_{1-x}Te$ nanoparticles from cluster **2a** (bottom), **2b** (middle), and **4** (top).

within these systems occupy surface positions on the nanoparticles. The calculated lattice constant $a = 6.45$ Å is very similar to that of bulk CdTe ($a = 6.48$ Å); however, the small disparity suggests that a small amount of zinc exists within the core (i.e., a concentration gradient). By Vegard's analogy,[47] lattice constants for $Zn_xCd_{1-x}Te$ ($x = 0.18$–0.27) should lie in the range of 6.38–6.42 Å in a homogeneously mixed system.

Particle growth and mechanistic considerations: The synthesis of CdSe and ZnSe nanoparticles was carried out by means of decomposition of the clusters $[M_{10}Se_4(SPh)_{16}][X]_4$ ($M = Cd$, $X = Li^+$; $M = Zn$, $X = Me_4N^+$).[9] In addition to the evident extension of this approach to ternary $Zn_xCd_{1-x}E$ nanomaterials, several notable differences in the constitution of the cluster precursors used here appear to have a significant influence on the growth pathway of the nanomaterials. The first apparent disparity arises from the metal-to-chalcogen ratio present in the molecules. While the ratio of metal-to-chalcogenide (E^{2-}) ligands is equivalent for all $\{M_{10}\}$ clusters, the presence of phenylselenolate and -tellurolate ligands in clusters **1** and **2** provide an additional source of E^{2-}. Indeed, studies of the solid-state thermolysis of clusters **1**–**4** have demonstrated that the stoichiometric formation of bulk and nanocrystalline $Zn_xCd_{1-x}E$ materials is accommodated by the generation of E^{2-} through the elimination of Ph_2E molecules.[19,20] Evidently, this pathway is not available for the generation of MSe materials from $[M_{10}Se_4(SPh)_{16}]^{4-}$. Thus, due to the high M/Se ratio in these clusters, the formation of nanoparticles must be accompanied by the elimination of metal ions. The authors suggest that the initial nucleus-formation step involves the elimination of $Cd(SPh)_3^-$ units from the apical positions, and that further nanoparticle growth additionally involves the formation of other cadmium thiophenolate or amine complexes.[9]

While this adequately accounts for the growth of CdSe nanoparticles from the $[M_{10}Se_4(SPh)_{16}]^{4-}$ precursors, it does not seem to be the most viable route to nanoparticle formation from clusters **1** and **2**. Primary evidence is provided by the observed retention of the metal-ion stoichiometry throughout the formation of the nanocrystalline products. NMR and crystallographic analysis have revealed that the metal distribution in the cluster complexes **1** and **2** is not homogeneous, but rather that the Zn^{II} ions predominantly occupy the apical positions on the clusters.[19b] The elimination of $M(SePh)_3^-$ from the terminal positions of these clusters would consequently result in a marked increase in the Cd/Zn ratio.

To further probe the cluster decomposition process, the HDA–nanoparticle mixtures were dissolved in CH_2Cl_2 and analyzed by GC/MS. In addition to the evidently ubiquitous presence of hexadecylamine and other long chain amines, the existence of organochalcogen complexes provided valuable information. For the decomposition of clusters **1a** and **1b**, reaction mixtures in the early stages of cluster growth (120–160 °C) invariably contain diphenyldiselenide (Ph_2Se_2). The relative concentration of Ph_2Se_2 in the reaction mixture slowly declines with increasing reaction temperature, and this decrease is complemented by the gradual appearance of diphenylselenide (Ph_2Se). The formation of $Zn_xCd_{1-x}Te$ nanomaterials from clusters **2a**,**b** appears to follow the same pathway, as Ph_2Te_2 is observed only at low reaction temperatures. The onset of Ph_2Te formation occurs at lower temperatures for the tellurium derivatives, consistent with the earlier onset of growth in these clusters.

For the adamantoid clusters **1**–**2**, it can be supposed that the first step of lyothermal decomposition involves the replacement of the $PnPr_3$ ligands at the terminal positions by simple mass action of the HDA to produce a $[Zn_xCd_{10-x}E_4(EPh)_{12}(HDA)_4]$ cluster. This is followed immediately by the elimination of (at least a portion of) the phenylchalcogenolate ligands to produce a metal-rich intermediate, with the resultant free sites on the metal atoms occupied by HDA ligands. Since reductive elimination of Ph_2E_2 ($E = Se$, Te) from the cluster framework is unlikely, the appearance of this species in the GC/MS may indicate the presence $[M(EPh)_2]$ or $[M(EPh)_3]^-$ complexes in the reaction mixture. If this is the case, however, such elimination must proceed such that the metal stoichiometry remains unchanged. An alternative explanation for the formation of Ph_2E_2 may involve the direct elimination of PhE^- from the cluster framework, followed by oxidation caused by ambient conditions in the reaction flask. Following the establishment of an M_xE_x core, further growth progression could occur through the Ostwald ripening process.

The mechanism outlined above is most likely an oversimplification of the actual thermodegradation process; however, it does satisfactorily account for the major differences between our investigations and earlier studies.[9] Although the formation of Ph_2S_2 from excess thiol has been speculated to occur in the lyothermal degradation of $[M_{10}Se_4(SPh)_{16}]^{4-}$, the corresponding conversion of this species to Ph_2S and S^{2-} can be ruled out by the observed formation of pure M_xSe_x nanoparticles. The differences in proposed reaction pathways can be attributed to the relative stability of E–E and E–C bonds, which decrease in the order $E = S > Se > Te$. The results of our investigations suggest that the substitution of −SPh ligands for −SePh or −TePh may afford the advantage of higher yields (c.f. the compulsory loss of 60 % of M^{II} centers from $[M_{10}Se_4(SPh)_{16}]^{4-}$).

Finally, the apparent concentration of Zn^{II} near the surface of the nanoparticles can be accounted for in terms of the relative strength of the metal–amine interaction. The anticipated stronger Zn–N interaction[48] may result in the continuous "extraction" of zinc to the surface. The distribution of metal ions within the nanoparticles appears to mirror that observed in the cluster precursors.[19] These results suggest that both composition and metal-ion distribution of the nanoparticles may be determined by the characteristics of the clusters themselves. Thus, this method thus affords a convenient route to ternary CdE/ZnE with core/shell-type architecture.

The effect of Zn^{II} ions at the surface during the lyothermal degradation process apparently slows the growth pro-

gression in these ternary systems (relative to CdSe[9]). This is consistent with the formation of ZnSe nanoparticles using $[Zn_{10}Se_4(SPh)_{16}]^{4-}$, in which the particle sizes reached a maximum at approximately 5 nm, although Hines and Guyot-Sionnest found that the use of a mixture of alkylamine and trioctylphosphine (versus TOP/TOPO) as the coordinating solvent afforded enhancement of the growth rate in the synthesis of ZnE nanocrystals.[49] The retarded growth was attributed to the strong coordination of TOPO to the Zn centers.

Conclusion

The lyothermal degradation of molecular metal–chalcogen cluster precursors represents a convenient route for the generation of larger nanocrystalline materials. This approach was utilized for the formation of ternary $Zn_xCd_{10-x}Se$ and $Zn_xCd_{1-x}Te$ nanoparticles from ternary cluster molecules. For the degradation of the adamantoid clusters $[Zn_xCd_{10-x}E_4(EPh)_{12}(PnPr_3)_4]$ (E = Se, Te; $x = 0.18$, 0.26), both the composition and metal-ion distribution of the clusters was reflected in the resultant nanocrystalline products, demonstrating that these clusters are efficient precursors for the formation of ternary materials. Thermolysis of the clusters $[Zn_5Cd_{11}Se_{13}(SePh)_6(N,N'\text{-tmeda})_5]$, on the other hand, resulted in partial loss of zinc. Spectroscopic and crystallographic data suggests an inhomogeneous distribution of the metal centers, with Zn ions evidently concentrated near the surfaces of the nanoparticles. The products were highly crystalline and featured a narrow size distribution, and the growth of the nanocrystals could be controlled by variation of the reaction temperature; however, the sizes were significantly smaller than those reported for CdSe nanoparticles obtained using a similar approach. Structural differences between the cluster precursors reported here and those used to generate binary CdSe[26] appear to have a significant effect on nanoparticle growth.

Experimental Section

Materials and methods: All synthetic preparations were carried out under an inert (N_2) atmosphere by using standard Schlenk techniques. Clusters **1**–**4** were synthesized by using previously reported procedures.[19–20] Hexadecylamine (tech, 90%) was purchased from Aldrich and used without further purification. HPLC grade toluene (Fisher Chemicals) and glass-distilled CH_2Cl_2 and methanol (Caledon) were used as provided. UV-visible spectroscopy was performed using a Varian Cary 100 Bio UV-visible spectrophotometer. Photoluminesence (PL) spectra were measured at room temperature by using a Photon Technology Quanta Master (QM4/2003) scanning spectrofluorimeter. PL measurements were conducted on dilute solutions in order to avoid self-absorption by the nanoparticles. Powder X-ray diffraction measurements were carried out on a Rigaku diffractometer with $Co_{K\alpha}$ radiation source ($\lambda =$ 1.799260 Å). Samples were prepared by placing finely dispersed powders on standard supports. Dynamic light-scattering experiments were carried out with a Malvern Zetasizer Nano S series particle size analyzer with a He-Ne laser (633 nm) and Avalanche photodiode photon detector. Solvents and samples were filtered through 0.1 μm Anotop 10 inorganic membrane filters (Whatman) prior to analysis. All measurements were recorded at 20 °C in quartz cuvettes. EDX analyses were carried out at Surface Science Western (Mr. Ross Davidson) with an EDAX Phoenix Model energy dispersive X-ray system that was coupled to a Hitachi S-4500 scanning electron microscope (SEM). Analyses were carried out by using a 20 kV electron beam rastered over a 100 × 100 μm area and measurements were conducted on multiple samples to ensure reproducibility. The samples for the TEM characterization were prepared by dropping a suspension of THF containing the samples onto carbon-coated copper grids. TEM investigations were performed in a Philips Tecnai F20 ST operated at 200 kV using an extraction voltage of 4.1 keV for the field emission gun. The point resolution of this microscope was about 0.235 nm at Scherzer focus and an information limit of about 0.14 nm was obtained. High-resolution micrographs were taken with a 1 × 1 K CCD camera and analyzed with the software package Digital Micrographs (Version 3.5.2, Gatan Company) in order to perform Fourier transformations.

Synthesis of the nanoparticles: The synthesis of ternary $Zn_xCd_{1-x}E$ nanoparticles from cluster precursors was carried out in a similar manner as reported previously for the synthesis of CdSe nanoparticles from $[Cd_{10}Se_4(SPh)_{16}][Li]_4$.[9] The typical preparations were as follows: Hexadecylamine (25 g) was dried and degassed in the reaction vessel by heating to 120 °C under vacuum for 60 min, during which time the flask was periodically flushed with nitrogen. The cluster complex (0.25 g) was added with stirring at 120 °C under a flow of N_2, and the flask was sealed with a septum. The reaction temperature was then raised slowly (~1 °C min^{-1}) and aliquots (~4 mL) were taken from the reaction mixture at various intervals. The hexadecylamine solidified upon standing at room temperature, providing a matrix in which the nanoparticle materials were stable for a short duration even under atmospheric conditions. The growth of the nanocrystalline materials was monitored by absorption spectroscopy. At the desired nanoparticle size, thermal annealing could be carried out by lowering the reaction temperature by 20–30 °C and holding at that temperature for several hours.

Isolation and purification of the nanoparticles: The ternary $Zn_xCd_{1-x}Se$ and $Zn_xCd_{1-x}Te$ nanoparticles were separated from the HDA by treating hot (~60 °C) solutions with anhydrous methanol followed by centrifugation. Excess HDA was removed by successive resuspension of the nanoparticles in methanol and isolated again by centrifugation. The solids were then dried under vacuum for 60 min.

Acknowledgements

The authors are grateful to the Natural Sciences and Engineering Research Council (NSERC) of Canada and the Government of Ontario's PREA program for financial support of this research. Equipment funding was provided by the Canadian Foundation for Innovation, The University of Western Ontario, and the NSERC. M.W.D. also thanks the NSERC for a post-graduate scholarship.

[1] C. B. Murray, D. J. Norris, M. G. Bawendi, *J. Am. Chem. Soc.* **1993**, *115*, 8706–8715.

[2] a) T. Trindade, P. O'Brien, X.-M. Zhang, *Chem. Mater.* **1997**, *9*, 523–530; b) B. Ludolph, M. A. Malik, P. O'Brien, N. Revaprasadu, *Chem. Commun.* **1998**, 1849–1850; c) N. Revaprasadu, M. A. Malik, P. O'Brien, M. M. Zulu, G. Wakefield, *J. Mater. Chem.* **1998**, *8*, 1885–1888; d) N. Revaprasadu, M. A. Malik, P. O'Brien, G. Wakefield, *J. Mater. Res.* **1999**, *14*, 3237–3240; e) M. Lazell, P. O'Brien, *Chem. Commun.* **1999**, 2041–2042; f) M. A. Malik, N. Revaprasadu, P. O'Brien, *Chem. Mater.* **2001**, *13*, 913–920.

[3] a) J. G. Brennan, T. Siegrist, P. J. Carroll, S. M. Stuczynski, L. E. Brus, M. L. Steigerwald, *J. Am. Chem. Soc.* **1989**, *111*, 4141–4143; b) M. L. Steigerwald, S. M. Stuczynski, Y. U. Kwon, D. A. Vennos, J. G. Brennan, *Inorg. Chim. Acta* **1993**, *212*, 219–224; c) M. L. Steigerwald, *Polyhedron* **1994**, *13*, 1245–1252, and references therein.

[4] a) Y.-W. Jun, J.-E. Koo, J. Cheon, *Chem. Commun.* **2000**, 1243–1244; b) Y.-W. Jun, C.-S. Choi, J. Cheon, *Chem. Commun.* **2001**, 101–102.
[5] N. L. Pickett, P. O'Brien, *Chem. Rec.* **2001**, *1*, 467–479.
[6] T. Trindade, P. O'Brien, N. L. Pickett, *Chem. Mater.* **2001**, *13*, 3843–3858.
[7] S. L. Stoll, A. G. Gillan, A. R. Barron, *Chem. Vap. Deposition* **1996**, *2*, 182–184.
[8] N. L. Pickett, S. Lawson, W. G. Thomas, F. G. Riddell, D. F. Foster, D. J. Cole-Hamilton, J. R. Fryer, *J. Mater. Chem.* **1998**, *8*, 2769–2776.
[9] S. L. Cumberland, K. L. Hanif, A. Javier, G. A. Khitrov, G. F. Strouse, S. M. Woessner, C. S. Yun, *Chem. Mater.* **2002**, *14*, 1576–1584.
[10] I. G. Dance, A. Choy, M. L. Scudder, *J. Am. Chem. Soc.* **1984**, *106*, 6285–6295.
[11] K. M. Hanif, R. W. Meulenberg, G. F. Strouse, *J. Am. Chem. Soc.* **2002**, *124*, 11495–11502.
[12] F. E. Osterloh, D. P. Hewitt, *Chem. Commun.* **2003**, 1700–1701.
[13] a) Z. A. Peng, X. Peng, *J. Am. Chem. Soc.* **2002**, *124*, 3343–3353; b) Z. A. Peng, X. Peng *J. Am. Chem. Soc.* **2001**, *123*, 1389–1395; c) L. Ou, Z. A. Peng, X. Peng, *Nano Lett.* **2001**, *1*, 333–337; d) J. E. B. Katari, V. L. Colvin, A. P. Alivisatos, *J. Phys. Chem.* **1994**, *98*, 4109–4117; e) X. Peng, J. Wickham, A. P. Alivisatos, *J. Am. Chem. Soc.* **1998**, *120*, 5343–5344; f) L. Manna, E. C. Scher, A. P. Alivisatos, *J. Am. Chem. Soc.* **2000**, *122*, 12700–12706.
[14] H.-J. Eisler, V. C. Sundar, M. G. Bawendi, M. Walsh, H. I. Smith, V. Klimov, *Appl. Phys. Lett.* **2002**, *80*, 4614–4616.
[15] a) W. Wang, I. Germanenko, M. S. El-Shall, *Chem. Mater.* **2002**, *14*, 3028–3033; b) B. A. Korgel, H. G. Monbouquette, *Langmuir* **2000**, *16*, 3588–3594; c) D. V. Petrov, B. S. Santos, G. A. L. Pereira, C. D. M. Donegá, *J. Phys. Chem. B* **2002**, *106*, 5325–5334.
[16] a) M. T. Harrison, S. V. Kershaw, M. G. Burt, A. Eychmüller, H. Weller, A. L. Rogach, *Mater. Sci. Eng. B* **2000**, *69*, 355–360; b) A. L. Rogach, M. T. Harrison, S. V. Kershaw, A. Kornowski, M. G. Burt, A. Eychmüller, H. Weller, *Phys. Status Solidi B* **2001**, *224*, 153–158.
[17] X. Zhong, S. Liu, Z. Zhang, L. Li, Z. Wei, W. Knoll, *J. Mater. Chem.* **2004**, *14*, 2790–2794.
[18] a) X. Zhong, M. Han, Z. Dong, T. J. White, W. Knoll, *J. Am. Chem. Soc.* **2003**, *125*, 8589–8594; b) X. Zhong, Z. Zhang, S. Liu, M. Han, W. Knoll, *J. Phys. Chem. B* **2004**, *108*, 15552–15559.
[19] a) M. W. DeGroot, J. F. Corrigan, *Angew. Chem.* **2004**, *116*, 5469–5471; *Angew. Chem. Int. Ed.* **2004**, *43*, 5355–5357; b) M. W. DeGroot, N. J. Taylor, J. F. Corrigan, *Inorg. Chem.* **2005**, *44*, 5447–5458.
[20] a) M. W. DeGroot, N. J. Taylor, J. F. Corrigan, *J. Am. Chem. Soc.* **2003**, *125*, 864–865; b) M. W. DeGroot, N. J. Taylor, J. F. Corrigan, *J. Mater. Chem.* **2004**, *14*, 654–660.
[21] A. P. Alivisatos, *J. Phys. Chem.* **1996**, *100*, 13226–13239.
[22] A. Henglein, *Chem. Rev.* **1989**, *89*, 1861–1873.
[23] H. Weller, *Angew. Chem.* **1993**, *105*, 43–55; *Angew. Chem. Int. Ed. Engl.* **1993**, *32*, 41–53.
[24] C. B. Murray, C. R. Kagan, M. G. Bawendi, *Annu. Rev. Mater. Sci.* **2000**, *30*, 545–610.
[25] M. A. El-Sayed, *Acc. Chem. Res.* **2004**, *37*, 326–333.
[26] A. L. Efros, M. Rosen, *Annu. Rev. Mater. Sci.* **2000**, *30*, 475–521.
[27] M. G. Bawendi, M. L. Steigerwald, L. E. Brus, *Annu. Rev. Phys. Chem.* **1990**, *41*, 477–496.
[28] a) R. Rossetti, R. Hull, J. M. Gibson, L. E. Brus, *J. Chem. Phys.* **1985**, *82*, 552–559; b) R. Rossetti, J. L. Ellison, J. M. Gibson, L. E. Brus, *J. Chem. Phys.* **1984**, *80*, 4464–4469.
[29] T. Inokuma, T. Arai, M. Ishikawa, *Phys. Rev. B* **1990**, *42*, 11093–11098.
[30] a) M. G. Bawendi, W. L. Wilson, L. Rothberg, P. J. Carrol, T. M. Jedju, M. L. Steigerwald, L. E. Brus, *Phys. Rev. Lett.* **1990**, *65*, 1623–1626; b) M. G. Bawendi, W. L. Wilson, P. J. Carrol, L. E. Brus, *J. Chem. Phys.* **1992**, *96*, 946–954.
[31] D. J. Norris, M. G. Bawendi, *Phys. Rev. B* **1996**, *53*, 16338–16346.
[32] P. Reiss, G. Quemard, S. Carayon, J. Bleuse, F. Chandezon, A. Pron, *Mater. Chem. Phys.* **2004**, *84*, 10–13.
[33] A. L. Rogach, *Mater. Sci. Eng. B* **2000**, *69–70*, 435–440.
[34] G. Ma, S.-H. Tang, W. Sun, Z. Shen, W. Huang, J. Shi, *Phys. Lett. A* **2002**, *299*, 581–585.
[35] J. Roither, W. Heiss, D. V. Talapin, N. Gaponik, A. Eychmuller, *Appl. Phys. Lett.* **2004**, *84*, 2223–2225.
[36] S. Krishnadasan, J. Tovilla, A. J. Vilar, A. J. deMello, J. C. deMello, *J. Mater. Chem.* **2004**, *14*, 2655–2660.
[37] D. L. Klein, R. Roth, A. K. L. Lim, A. P. Alivisatos, P. L. McEuen, *Nature*, **1997**, *389*, 699–701.
[38] S. C. Lee, R. H. Holm, *Angew. Chem.*, **1990**, *102*, 868–885; *Angew. Chem. Int. ed. Engl.* **1990**, *29*, 840–857.
[39] J. F. Corrigan, M. W. DeGroot in *The Chemistry of Nanomaterials: Synthesis, Properties and Applications* (Eds.: C. N. R. Rao, A. Müller, A. K. Cheetham), Wiley-VCH, Weinheim, **2004**, pp. 418–451.
[40] a) A. Choy, D. C. Craig, I. G. Dance, M. L. Scudder, *J. Chem. Soc. Chem. Commun.* **1982**, 1246–1247; b) I. G. Dance, A. Choy, M. L. Scudder, *J. Am. Chem. Soc.* **1984**, *106*, 6285–6295; c) M. D. Nyman, M. J. Hampden-Smith, E. N. Duesler, *Inorg. Chem.* **1996**, *35*, 802–803; d) R. D. Adams, B. Zhang, C. J. Murphy, L. K. Yeung, *Chem. Commun.* **1999**, 383–384.
[41] a) A. Eichhöfer, A. Aharoni, U. Banin, *Z. Anorg. Allg. Chem.* **2002**, *628*, 2415–2421; b) A. Eichhöfer, E. Tröster, *Eur. J. Inorg. Chem.* **2002**, 2253–2256; c) Eichhöfer, P. Deglmann, *Eur. J. Inorg. Chem.* **2004**, 349–355; d) A. Eichhöfer, D. Fenske, H. Pfistner, M. Wunder, *Z. Anorg. Allg. Chem.* **1998**, *624*, 1909–1914; e) H. Pfistner, D. Fenske, *Z. Anorg. Allg. Chem.* **2001**, *627*, 575–582; f) S. Behrens, M. Bettenhausen, A. Eichhöfer, D. Fenske, *Angew. Chem.* **1997**, *109*, 2874–2876; *Angew. Chem. Int. Ed. Engl.* **1997**, *36*, 2797–2798.
[42] a) M. Danek, K. F. Jensen, C. B. Murray, M. G. Bawendi, *Chem. Mater.* **1996**, *8*, 173–180; b) X. Peng, M. C. Schlamp, A. V. Kadavanich, A. P. Alivisatos, *J. Am. Chem. Soc.* **1997**, *119*, 7019–7029; c) J. Rodríguez-Viejo, H. Mattousi, J. R. Heine, M. K. Kuno, J. Michel, M. G. Bawendi, K. F. Jensen, *J. Appl. Phys.* **2000**, *87*, 8526–8534; d) B. O. Dabbousi, J. Rodríguez-Viejo, F. V. Mikulec, J. R. Heine, H. Mattoussi, R. Ober, K. F. Jensen, M. G. Bawendi, *J. Phys. Chem. B* **1997**, *101*, 9463–9475; e) U. Banin, M. Bruchez, A. P. Alivisatos, T. Ha, S. Weiss, D. S. Chemla, *J. Chem. Phys.* **1999**, *110*, 1195–1201.
[43] a) A. Hässelbarth, A. Eychmüller, H. Weller, *J. Lumin.* **1992**, *53*, 113–115; b) A. Hässelbarth, A. Eychmüller, R. Eichburger, M. Giesi, A. Mews, H. Weller, *J. Phys. Chem.* **1993**, *97*, 5333–5340; c) D. V. Talapin, A. L. Rogach, A. Kornowski, M. Haase, H. Weller, *Nano Lett.* **2001**, *1*, 207–211; d) I. Mekis, D. V. Talapin, A. Kornowski, M. Haase, H. Weller, *J. Phys. Chem. B* **2003**, *107*, 7454–7462; e) D. V. Talapin, R. Koeppe, S. Götzinger, A. Kornowski, J. M. Lupton, A. L. Rogach, O. Benson, J. Feldmann, H. Weller, *Nano Lett.* **2003**, *3*, 1677–1681.
[44] a) M. A. Malik, P. O'Brien, N. Revaprasadu, *Chem. Mater.* **2002**, *14*, 2004–2010; b) M. A. Hines, P. Guyot-Sionnest, *J. Phys. Chem.* **1996**, *100*, 468–471; c) Y. Tian, T. Newton, N. A. Kotov, D. M. Guldi, J. H. Fendler, *J. Phys. Chem.* **1996**, *100*, 8927–8939; d) W. G. J. H. M. van Sark, P. L. T. M. Frederix, D. J. Van den Heuvel, H. C. Gerritsen, A. A. Bol, J. N. J. van Lingen, C. de Mello Donegá, A. Meijerink, *J. Phys. Chem. B* **2001**, *105*, 8281–8284.
[45] a) S. Kim, B. Fisher, H.-J. Eisler, M. Bawendi, *J. Am. Chem. Soc.* **2003**, *125*, 11466–11467; b) A. Mews, A. Eychmüller, M. Giersig, D. Schooss, H. Weller, *J. Phys. Chem.* **1994**, *98*, 934–941; c) M. Braus, C. Burda, M. A. E1-Sayed, *J. Phys. Chem. A* **2001**, *105*, 5548–5551; d) D. Battaglia, J. J. Li, Y. Wang, X. Peng, *Angew. Chem.* **2003**, *115*, 5189–5193; *Angew. Chem. Int. Ed.* **2003**, *42*, 5035–5039.
[46] X. Zhong, R. Xie, Y. Zhang, T. Basché, W. Knoll, *Chem. Mater.* **2005**, *17*, 4038–4042.
[47] L. Vegard, *Z. Phys.* **1921**, *5*, 17–26.
[48] I. E. Gumrukcuoglu, J. Jeffery, M. F. Lappert, J. B. Pedley, A. K. Rai, *J. Organomet. Chem.* **1988**, *341*, 53–62.
[49] M. A. Hines, P. Guyot-Sionnest, *J. Phys. Chem. B* **1998**, *102*, 3655–3657.

Received: September 1, 2005
Published online: November 30, 2005

